PHYSICAL REVIEW D **87,** 057502 (2013)

Description of the $\psi(3770)$ resonance interfering with the background

N. N. Achasov* and G. N. Shestakov†

Laboratory of Theoretical Physics, S.L. Sobolev Institute for Mathematics, 630090 Novosibirsk, Russia

(Received 18 February 2013; published 25 March 2013)

The parameters of the interfering $\psi(3770)$ resonance should be determined from the data on the reactions $e^+e^- \to D\bar{D}$ with the use of the models satisfying the elastic unitarity requirement. The selection of such models can be realized by comparing their predictions with the relevant data on the shape of the $\psi(3770)$ peak in the non-$D\bar{D}$ decay channels. Here, we illustrate this unitarity approach by the example of the most simple variant of the model of the mixed $\psi(3770)$ and $\psi(2S)$ resonances. When new high-statistics data become available, it will be interesting to test this clarity variant.

DOI: 10.1103/PhysRevD.87.057502 PACS numbers: 13.25.Gv, 13.40.Gp, 13.66.Jn

In the recent paper [1], we considered a few unitarized models available for phenomenological description of the $e^+e^- \to D\bar{D}$ reaction cross section in the $\psi(3770)$ resonance region. Such models allow us to avoid the spurious ambiguities in the interfering $\psi(3770)$ resonance parameters determination, which have been recently revealed by experimentalists when using unitarily uncorrected parametrizations [2–6].

In this report we present the simplest working variant of the model of the mixed $\psi(3770)$ and $\psi(2S)$ resonances for the description of interference phenomena in the $\psi(3770)$ region. It was not discussed in Ref. [1]. Owing to own clarity and simplicity this variant can be tested, in the first place, in the treatment of new high-statistics data which can be expected from CLEO-c and BESIII [5,7–11] on the $\psi(3770)$ shape in $e^+e^- \to D\bar{D}$. Here we also concentrate great attention on the possibility of testing theoretical models by comparing their predictions with the relevant data on the shape of the $\psi(3770)$ peak in the non-$D\bar{D}$ decay channels, which are also expected from BESIII [9–11].

In constructing the model describing the process $e^+e^- \to D\bar{D}$, one must keep in mind that we investigate above all the D-meson isoscalar electromagnetic form factor F_D^0. The phase of F_D^0 in the elastic region [i.e., between the $D\bar{D}$ (≈ 3.739 GeV) and $D\bar{D}^*$ (≈ 3.872 GeV) thresholds] is fixed by the unitarity condition equal to the phase δ_1^0 of the strong P-wave $D\bar{D}$ scattering amplitude T_1^0 in the channel with isospin $I = 0$, i.e.,

$$F_D^0 = e^{i\delta_1^0}\mathcal{F}_D^0, \tag{1}$$

where $\mathcal{F}_D^0$ and δ_1^0 are the real functions of energy. A similar representation of the amplitude $e^+e^- \to D\bar{D}$ used for the data description guarantees the unitarity requirement on the model level [1]. The sum of the $e^+e^- \to D\bar{D}$ reaction cross sections is given by

$$\sigma(e^+e^- \to D\bar{D}) = \frac{8\pi\alpha^2}{3s^2}|F_D^0(s)|^2\nu(s), \tag{2}$$

where s is the $D\bar{D}$-pair invariant mass square, $\nu(s) = [p_0^3(s) + p_+^3(s)]/\sqrt{s}$, $p_{0,+}(s) = \sqrt{s/4 - m_{D^{0,+}}^2}$ and $\alpha = e^2/4\pi = 1/137$ (here we do not touch on the questions about the isospin symmetry breaking). Below, for short $\psi(3770)$ is denoted as ψ''.

Consider now the model which takes into account in F_D^0 and T_1^0 the contributions only from the ψ'' and $\psi(2S)$ resonances. Owing to the common $D^0\bar{D}^0$ and D^+D^- coupled channels, the ψ'' and the $\psi(2S)$ can transform into each other (i.e., mix); for example, $\psi'' \to D\bar{D} \to \psi(2S)$. The form factor F_D^0, corresponding to the contribution of the mixed ψ'' and $\psi(2S)$ resonances, can be represented in the following symmetric form [1,12–14]:

$$F_D^0(s) = \frac{\mathcal{R}_{D\bar{D}}(s)}{D_{\psi''}(s)D_{\psi(2S)}(s) - \Pi_{\psi''\psi(2S)}^2(s)}, \tag{3}$$

where $D_{\psi''}(s)$ and $D_{\psi(2S)}(s)$ are the inverse propagators of ψ'' and $\psi(2S)$, respectively,

$$D_{\psi''}(s) = m_{\psi''}^2 - s - i\sqrt{s}\Gamma_{\psi''D\bar{D}}(s), \tag{4}$$

$$D_{\psi(2S)}(s) = m_{\psi(2S)}^2 - s - i\sqrt{s}\Gamma_{\psi(2S)D\bar{D}}(s), \tag{5}$$

$$\Gamma_{\psi''D\bar{D}}(s) = \frac{g_{\psi''D\bar{D}}^2}{6\pi}\frac{\nu(s)}{\sqrt{s}}, \tag{6}$$

$$\Gamma_{\psi(2S)D\bar{D}}(s) = \frac{g_{\psi(2S)D\bar{D}}^2}{6\pi}\frac{\nu(s)}{\sqrt{s}}, \tag{7}$$

$$\begin{aligned}\mathcal{R}_{D\bar{D}}(s) = {} & g_{\psi(2S)\gamma}[D_{\psi''}(s)g_{\psi(2S)D\bar{D}} + \Pi_{\psi''\psi(2S)}(s)g_{\psi''D\bar{D}}] \\ & + g_{\psi''\gamma}[D_{\psi(2S)}(s)g_{\psi''D\bar{D}} \\ & + \Pi_{\psi''\psi(2S)}(s)g_{\psi(2S)D\bar{D}}].\end{aligned} \tag{8}$$

The constants $g_{\psi''D\bar{D}}$, $g_{\psi(2S)D\bar{D}}$, and $g_{\psi''\gamma}$, $g_{\psi(2S)\gamma}$ characterize couplings of the ψ'', $\psi(2S)$ to the $D\bar{D}$ and virtual γ quantum, respectively. The amplitude $\Pi_{\psi''\psi(2S)}(s)$ describing the $\psi'' - \psi(2S)$ mixing has the form

*achasov@math.nsc.ru
†shestako@math.nsc.ru

$$\Pi_{\psi''\psi(2S)}(s) = \mathrm{Re}\Pi_{\psi''\psi(2S)}(s) + i\frac{g_{\psi''D\bar{D}}g_{\psi(2S)D\bar{D}}}{6\pi}\nu(s). \tag{9}$$

Its imaginary part is due to the $\psi'' \to D\bar{D} \to \psi(2S)$ transitions via the real $D\bar{D}$ intermediate states. Substituting Eqs. (4)–(7) and (9) into Eq. (8), it is easy to make certain that $\mathcal{R}_{D\bar{D}}(s)$ is a real function. Thus, the model can explain the dip observed in $\sigma(e^+e^- \to D\bar{D})$ near $\sqrt{s} \approx 3.81$ GeV (see Fig. 1) by the zero in $F_D^0(s)$, caused by compensation between the ψ'' and $\psi(2S)$ contributions. Note that $\mathrm{Re}\Pi_{\psi''\psi(2S)}(s)$ cannot be strictly calculated. Its approximations, for example, by the expression $c_0 + sc_1$, where c_0 and c_1 are free parameters, can be used as a resource for the fit improvement. Below, for simplicity we put $\mathrm{Re}\Pi_{\psi''\psi(2S)}(s) = 0$. Then Eq. (8) takes the form

$$\mathcal{R}_{D\bar{D}}(s) = (m_{\psi''}^2 - s)g_{\psi(2S)\gamma}g_{\psi(2S)D\bar{D}} + (m_{\psi(2S)}^2 - s)g_{\psi''\gamma}g_{\psi''D\bar{D}}. \tag{10}$$

The curves in Fig. 1 correspond to $m_{\psi''} = 3.794$ GeV, $g_{\psi''D\bar{D}} = \pm 14.35$ [i.e., $\Gamma_{\psi''D\bar{D}}(m_{\psi''}^2) \approx 56.8$ MeV, see Eq. (6)], $g_{\psi''\gamma} = \pm 0.1234$ GeV^2 [i.e., $\Gamma_{\psi''e^+e^-} = 4\pi\alpha^2 g_{\psi''\gamma}^2/(3m_{\psi''}^3) \approx 0.062$ keV], and $g_{\psi(2S)D\bar{D}} = \pm 20.11$. In so doing, if $g_{\psi''\gamma}g_{\psi''D\bar{D}} > 0$ (< 0), then $g_{\psi(2S)\gamma}g_{\psi(2S)D\bar{D}} < 0$ (> 0), see Eq. (10). The values $m_{\psi(2S)} = 3.6861$ GeV and $g_{\psi(2S)\gamma} = \pm 0.7262$ GeV^2 were fixed according the data [6] and the relation $\Gamma_{\psi(2S)e^+e^-} = 4\pi\alpha^2 g_{\psi(2S)\gamma}^2/(3m_{\psi(2S)}^3) = 2.35$ keV.

The values of the fitted parameters $m_{\psi''}$, $g_{\psi''D\bar{D}}$, and $g_{\psi''\gamma}$ can essentially depend on the model used for the description of the total contribution of the ψ'' resonance and background. The analysis [1] indicates that the components of the $e^+e^- \to D\bar{D}$ amplitude can be very different in the different models. For the model of the mixed ψ'' and $\psi(2S)$ resonances, the contributions of the components in question are shown in Fig. 1 by the dashed and dot-dashed curves. On the other hand, it is clear that the interference pattern in the ψ'' region depends on the reaction. Therefore, the selection of the theoretical models should be carry out by comparing their predictions with the experimental data on the shape of the ψ'' peak for several different reactions.

For example, after the fitting of the $e^+e^- \to D\bar{D}$ data we all know about $D\bar{D}$ elastic scattering in the P-wave at the model level,

$$T_1^0(s) = e^{i\delta_1^0(s)}\sin\delta_1^0(s) = \frac{\nu(s)}{6\pi}\left[\frac{(m_{\psi''}^2 - s)g_{\psi(2S)D\bar{D}}^2 + (m_{\psi(2S)}^2 - s)g_{\psi''D\bar{D}}^2}{D_{\psi''}(s)D_{\psi(2S)}(s) - \Pi_{\psi''\psi(2S)}^2(s)}\right]. \tag{11}$$

The corresponding cross section and phase are shown in Fig. 2. Unfortunately, these predictions are not possible to verify. However, there are other processes which can be measured experimentally.

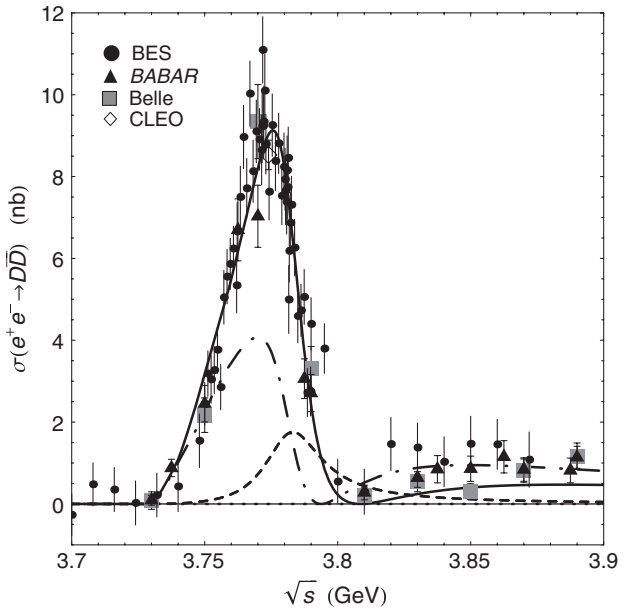

FIG. 1. The simplest variant of the model of the mixed ψ'' and $\psi(2S)$ resonances. The solid curve is the fit using Eqs. (2)–(10) to the data from BES [24,25], CLEO [26], *BABAR* [27,28], and Belle [29] for $\sigma(e^+e^- \to D\bar{D})$. The dashed and dot-dashed curves show the contributions to the cross section from the ψ'' and $\psi(2S)$ production amplitudes proportional to the products of the coupling constants $g_{\psi''\gamma}g_{\psi''D\bar{D}}$ and $g_{\psi(2S)\gamma}g_{\psi(2S)D\bar{D}}$, respectively; see Eqs. (3) and (10). For more details on the data see Ref. [1].

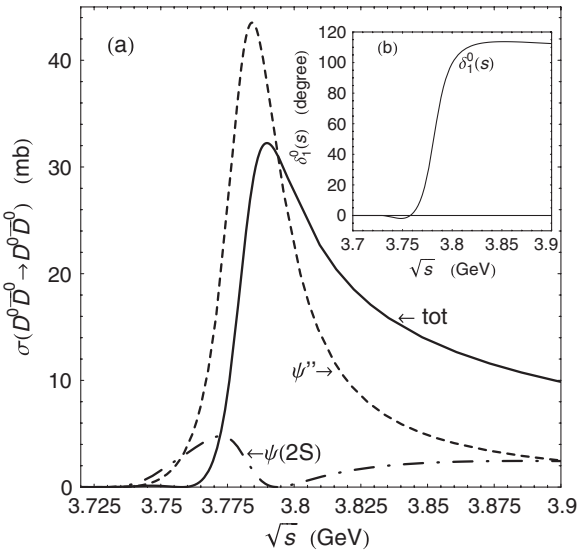

FIG. 2. The predictions of the model with the mixed ψ'' and $\psi(2S)$ resonances. (a) The solid, dashed, and dot-dashed curves correspond to $\sigma(D^0\bar{D}^0 \to D^0\bar{D}^0) = 3\pi|\sin\delta_1^0(s)|^2/p_0^2(s)$ and the ψ'' and $\psi(2S)$ contributions proportional to $g_{\psi''D\bar{D}}^2$ and $g_{\psi(2S)D\bar{D}}^2$ in Eq. (11), respectively. (b) The phase $\delta_1^0(s)$.

We are interested in the interference phenomena in the ψ'' region in the reactions $e^+e^- \to$ non-$D\bar{D}$. We confine ourselves to the simplest non-$D\bar{D}$ final states, the form factors of which are determined by a single independent invariant amplitude. Such reactions are $e^+e^- \to \gamma\chi_{c0}$, $\gamma\eta_c$, $\gamma\eta'$, $J/\psi\eta$, $\phi\eta$, and so on.

The cross section for $e^+e^- \to ab$ ($ab = \gamma\chi_{c0}$, $\gamma\eta_c$, $\gamma\eta'$, $J/\psi\eta$, $\phi\eta$) in the ψ'' region can be written as

$$\sigma(e^+e^- \to ab) = \frac{4\pi\alpha^2 k_{ab}^3(s)}{3s^{3/2}}|F_{ab}(s)|^2, \qquad (12)$$

where $k_{ab}(s) = \sqrt{[s-(m_a+m_b)^2][s-(m_a-m_b)^2]}/(2\sqrt{s})$ and $F_{ab}(s)$ is the electromagnetic form factor of the ab system. Equation (12) implies that the decay amplitude of the virtual timelike photon with the mass $\sqrt{s}$ into $\gamma\chi_{c0}$ (χ_{c0} is the scalar meson) is given by

$$eF_{\gamma\chi_{c0}}(s)\epsilon_\mu^\gamma(q)\epsilon_\nu^\gamma(k)(q\cdot k g_{\mu\nu} - k_\mu q_\nu), \qquad (13)$$

where $\epsilon_\mu^\gamma(q)$ and $\epsilon_\nu^\gamma(k)$ are the polarization four-vectors of the intermediate (virtual) and final photons with four-momenta q ($q^2 = s$) and k, respectively; and, its decay amplitude into $V0^-$ (0^- denotes a pseudoscalar meson and $V0^- = \gamma\eta_c$, $\gamma\eta'$, $J/\psi\eta$, $\phi\eta$) is given by

$$eF_{V0^-}(s)\varepsilon_{\mu\nu\sigma\tau}\epsilon_\mu^\gamma(q)\epsilon_\nu^V(k)q_\sigma k_\tau. \qquad (14)$$

In the model under consideration we may write

$$F_{ab}(s) = \frac{\mathcal{R}_{ab}(s)}{D_{\psi''}(s)D_{\psi(2S)}(s) - \Pi^2_{\psi''\psi(2S)}(s)}, \qquad (15)$$

where

$$\mathcal{R}_{ab}(s) = g_{\psi(2S)\gamma}[D_{\psi''}(s)g_{\psi(2S)ab} + \Pi_{\psi''\psi(2S)}(s)g_{\psi''ab}] + g_{\psi''\gamma}[D_{\psi(2S)(s)}g_{\psi''ab} + \Pi_{\psi''\psi(2S)}(s)g_{\psi(2S)ab}], \qquad (16)$$

and $g_{\psi(2S)ab}$, $g_{\psi''ab}$ are the effective coupling constants of the $\psi(2S)$, ψ'' to the ab channel. These coupling constants are taken into account in $F_{ab}(s)$ in the first order of perturbation theory. Their relative smallness is caused by the electromagnetic interaction for the $\gamma\chi_{c0}$ and $\gamma\eta_c$ channels, by the dynamics of the Okubo-Zweig-Iizuka rule violation [15–17] for the $J/\psi\eta$ and $\phi\eta$ channels, and by a combination of the above reasons for the $\gamma\eta'$ channel.

As a first (rough) approximation, we suppose that the coupling constants for radiative transitions between charmonium states $(c\bar{c})_i \to \gamma(c\bar{c})_f$ [index i (f) labels initial (final) state] and also those for hadronic transitions $(c\bar{c})_i \to (c\bar{c})_f h$ and radiative decays $(c\bar{c})_i \to \gamma h$, probing the gluon content of light hadrons h, are real [9,11,18]. That is, we neglect the contributions of the real $D\bar{D}$ intermediate states, taking into account which leads to the appearance of imaginary parts of effective coupling constants [15–17]. High-statistics studies of the $e^+e^- \to$ non-$D\bar{D}$ processes in the ψ'' region will show how this is justified. Note that for the $(c\bar{c})_i \to \phi\eta$ decay the $D\bar{D}$ loop rescattering mechanism $(c\bar{c})_i \to D\bar{D} \to \phi\eta$ is suppressed by the Okubo-Zweig-Iizuka rule. The phase of the $\phi\eta$ final state interaction is unknown. However, this phase is common for different contributions to $e^+e^- \to \phi\eta$ and does not appear in the cross section. At this stage, we do not take into account the interference between the $e^+e^- \to (c\bar{c}) \to \phi\eta$ amplitude and the background from the light quark production $e^+e^- \to (s\bar{s}) \to \phi\eta$. With the above assumptions, the effective coupling constants $g_{\psi(2S)\phi\eta}$ and $g_{\psi''\phi\eta}$ will be considered to be real as well.

Table I presents information about the $\psi(2S)$ [6] and ψ'' [6,19–22] resonances in the ab decay channels, which we use to construct the corresponding mass spectra. The values for $g_{\psi(2S)ab}$ indicated in the table are obtained, up to the sign, from the data on the $\psi(2S) \to ab$ decay widths by the formula

$$\Gamma_{\psi(2S)ab} = \frac{g^2_{\psi(2S)ab}}{12\pi}k^3_{ab}(m^2_{\psi(2S)}), \qquad (17)$$

which implies that the amplitudes of the $\psi(2S) \to \gamma\chi_{c0}$ and $\psi(2S) \to V0^-$ decays have the form

$$g_{\psi(2S)\gamma\chi_{c0}}\epsilon_\mu^{\psi(2S)}(q)\epsilon_\nu^\gamma(k)(q\cdot k g_{\mu\nu} - k_\mu q_\nu) \quad \text{and}$$
$$g_{\psi(2S)V0^-}\varepsilon_{\mu\nu\sigma\tau}\epsilon_\mu^{\psi(2S)}(q)\epsilon_\nu^V(k)q_\sigma k_\tau,$$

respectively. The relative signs of the constants $g_{\psi(2S)ab}$ and $g_{\psi''ab}$ are unknown. Therefore, the relative signs between the first and subsequent three terms in Eq. (16) (they are controlled by signs of the coupling constant products)

TABLE I. Information about the $\psi(2S)$ [6] and ψ'' [6,19–22] resonances in non-$D\bar{D}$ decay channels (ab).

ab	$B(\psi(2S) \to ab)$	$\Gamma_{\psi(2S)ab}$ (keV)	$g_{\psi(2S)ab}$ (GeV^{-1})	$B(\psi'' \to ab)$	$\Gamma_{\psi''ab}$ (keV)	$\sigma(e^+e^- \to ab)$ (pb)
$\gamma\chi_{c0}$	$(9.68 \pm 0.31)\%$	29.4 ± 0.9	$\pm(0.250 \pm 0.004)$	$(7.3 \pm 0.9) \times 10^{-3}$	172 ± 30	72 ± 9
$\gamma\eta_c$	$(3.4 \pm 0.5) \times 10^{-3}$	1.03 ± 0.15	$\pm(1.22 \pm 0.09) \times 10^{-2}$	$\cdots$	$\cdots$	$\cdots$
$\gamma\eta'$	$(1.23 \pm 0.06) \times 10^{-4}$	0.374 ± 0.018	$\pm(1.67 \pm 0.04) \times 10^{-3}$	$<1.8 \times 10^{-4}$	$\cdots$	$\cdots$
$J\psi\eta$	$(3.28 \pm 0.07)\%$	9.97 ± 0.21	$\pm(0.218 \pm 0.002)$	$(9 \pm 4) \times 10^{-4}$	21 ± 10	5.5 ± 2.5
$\phi\eta$	$(2.8^{+1.0}_{-0.8}) \times 10^{-5}$	$(8.5^{+3.0}_{-2.4}) \times 10^{-3}$	$\pm(2.7^{+0.5}_{-0.4}) \times 10^{-4}$	$(3.1 \pm 0.7) \times 10^{-4}$	7.4 ± 1.6	2.4 ± 0.6

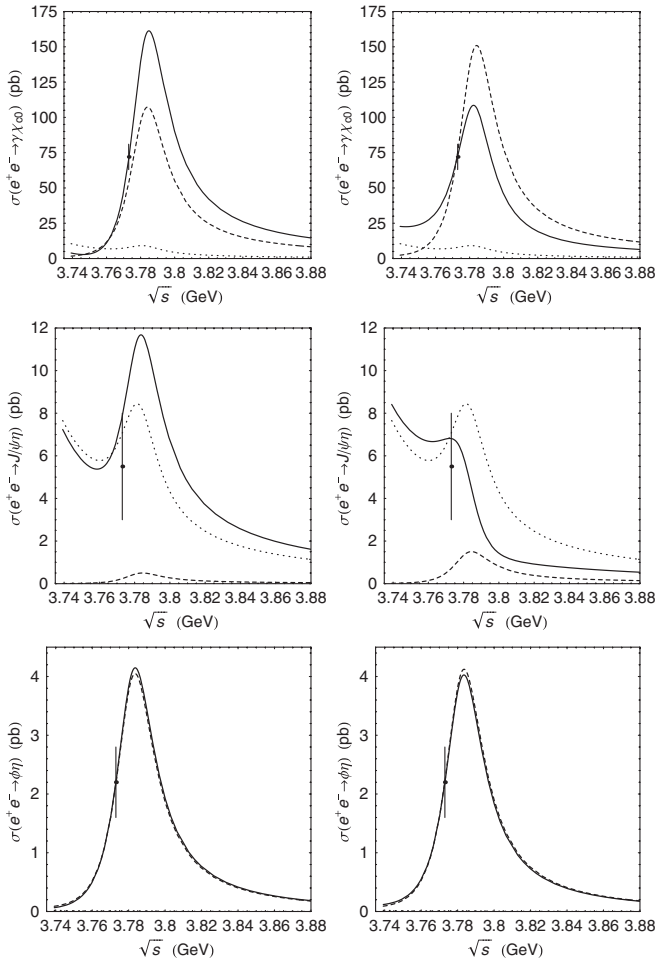

FIG. 3. The cross sections for $e^+e^- \to \gamma\chi_{c0}$, $e^+e^- \to J/\psi\eta$, and $e^+e^- \to \phi\eta$ (left) for case $(+\,-\,+)$ and (right) for case $(-\,+\,-)$.

can be chosen in two ways: $(+\,-\,+)$ or $(-\,+\,-)$. Here, we took into account the above-mentioned sign correlation between $g_{\psi''\gamma}g_{\psi''D\bar{D}}$ and $g_{\psi(2S)\gamma}g_{\psi(2S)D\bar{D}}$.

The existing information about the $\psi'' \to \gamma\chi_{c0}$, $\gamma\eta_c$, $\gamma\eta'$, $J/\psi\eta$, $\phi\eta$ decays are very poor. The CLEO Collaboration measured the reactions $e^+e^- \to \gamma\chi_{c0}$ [19], $e^+e^- \to J/\psi\eta$ [21], and $e^+e^- \to \phi\eta$ [22] at a single point in energy $\sqrt{s} = 3773$ MeV (at the supposed maximum of cross sections). The approximate values for $\sigma(e^+e^- \to ab)$ are presented in Table I and Fig. 3 by the points with the error bars. They allow us to roughly estimate the coupling constants $g_{\psi''\gamma\chi_{c0}} \approx \pm 0.608\ \mathrm{GeV}^{-1}$, $g_{\psi''J/\psi\eta} \approx \pm 0.0375\,\mathrm{GeV}^{-1}$, $g_{\psi''\phi\eta} \approx \pm 1.1 \times 10^{-2}\,\mathrm{GeV}^{-1}$ for case $(+\,-\,+)$ and $g_{\psi''\gamma\chi_{c0}} \approx \pm 0.721\ \mathrm{GeV}^{-1}$, $g_{\psi''J/\psi\eta} \approx \pm 0.065\,\mathrm{GeV}^{-1}$, $g_{\psi''\phi\eta} \approx \pm 1.11 \times 10^{-2}\,\mathrm{GeV}^{-1}$ for case $(-\,+\,-)$ by using Eqs. (12), (15), and (16), and construct the corresponding cross sections as functions of energy.

The solid curves in Fig. 3 show the cross sections for $e^+e^- \to \gamma\chi_{c0}$, $e^+e^- \to J/\psi\eta$, and $e^+e^- \to \phi\eta$; the dashed and dotted curves show the contributions from the ψ'' and $\psi(2S)$ resonances proportional to [see Eq. (16)]

$$[g_{\psi''\gamma}D_{\psi(2S)}(s) + g_{\psi(2S)\gamma}\Pi_{\psi''\psi(2S)}(s)]g_{\psi''ab} \quad \text{and}$$
$$[g_{\psi(2S)\gamma}D_{\psi''}(s) + g_{\psi''\gamma}\Pi_{\psi''\psi(2S)}(s)]g_{\psi(2S)ab},$$

respectively. The values of each of these contributions to $F_{ab}(s)$ change from reaction to reaction according to changes of $g_{\psi''ab}$ and $g_{\psi(2S)ab}$. At the same time, their s-dependence does not change, as it has already been determined by the model parameters found from fitting the $e^+e^- \to D\bar{D}$ cross section (simultaneous fits to the data on the reactions $e^+e^- \to D\bar{D}$ and $e^+e^- \to$ non-$D\bar{D}$ is yet to come). Note that the cross section for $e^+e^- \to \phi\eta$ is completely dominated by the ψ'' contribution. Note also that the Belle Collaboration has recently measured the cross section for $e^+e^- \to J/\psi\eta$ between $\sqrt{s} = 3.8$ GeV and 5.3 GeV [23]. Unfortunately, the data for 3.8 GeV $< \sqrt{s} < 4$ GeV have large errors, which does not allow us to extract any useful information.

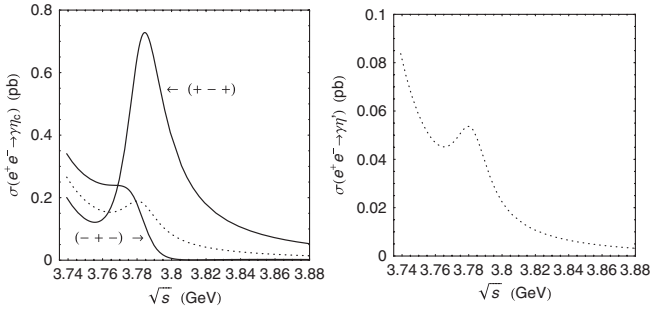

FIG. 4. The cross sections for $e^+e^- \to \gamma\eta_c$ (left) and $e^+e^- \to \gamma\eta'$ (right).

The cross sections for $e^+e^- \to \gamma\eta_c$ and $e^+e^- \to \gamma\eta'$ in the ψ'' region are unknown. Using information about the $\psi(2S)$ from Table I, we estimate the cross sections at $g_{\psi''\gamma\eta_c} = g_{\psi''\gamma\eta'} = 0$. The results are shown in Fig. 4 by the dotted curves. Here, as in the case of the dotted curves in Fig. 3, the resonant enhancement on the tails of the $\psi(2S)$ contribution arises owing to the $\psi'' - \psi(2S)$ mixing. If we put $\Gamma_{\psi''\gamma\eta_c} \approx 1$ keV [18], which corresponds to $g_{\psi''\gamma\eta_c} \approx \pm 1 \times 10^{-2}$ GeV^{-1}, then $\sigma(e^+e^- \to \gamma\eta_c)$ takes the form shown in the left plot in Fig. 4 by the solid curves for cases $(+\,-\,+)$ and $(-\,+\,-)$.

The above examples tell us that the mass spectra in the ψ'' region in the non-$D\bar{D}$ channels can be very diverse. Therefore, we should expect that the data on such spectra, together with the $e^+e^- \to D\bar{D}$ data, will impose severe restrictions on the constructed dynamical models for the ψ'' resonance interfering with the background.

This work was supported in part by RFBR, Grant No. 13-02-00039, and Interdisciplinary Project No. 102 of the Siberian division of RAS.

[1] N. N. Achasov and G. N. Shestakov, Phys. Rev. D **86**, 114013 (2012).
[2] A. D. Bukin, arXiv:0710.5627.
[3] K. Yu. Todyshev, http://phipsi11.inp.nsk.su/program.php.
[4] V. V. Anashin *et al.*, Phys. Lett. B **711**, 292 (2012).
[5] H.-B. Li, in *Proceedings of the 25th International Symposium on Lepton Photon Interactions at High Energies, 2011, Mumbai, India* [Pramana 79, 579 (2012)].
[6] J. Beringer *et al.* (Particle Data Group), Phys. Rev. D **86**, 010001 (2012).
[7] H.-B. Li, in *Proceedings of 14th International Conference on Hadron Spectroscopy (hadron 2011), Munich, 2011*, edited by B. Grube, S. Paul, and N. Brambilla, econf C110613 (2011).
[8] G. Huang, arXiv:1209.4813.
[9] D. M. Asner *et al.*, Int. J. Mod. Phys. A **24**, 499 (2009).
[10] G. Rong, D. Zhang, and J. C. Chen, arXiv:1003.3523.
[11] N. Brambilla *et al.*, Eur. Phys. J. C **71**, 1534 (2011).
[12] N. N. Achasov, S. A. Devyanin, and G. N. Shestakov, Phys. Lett. **88B**, 367 (1979).
[13] N. N. Achasov and G. N. Shestakov, Phys. Rev. D **58**, 054011 (1998).
[14] N. N. Achasov and A. A. Kozhevnikov, Phys. Rev. D **83**, 113005 (2011).
[15] N. N. Achasov and A. A. Kozhevnikov, Phys. Lett. B **260**, 425 (1991); Pis'ma Zh. Eksp Teor. Fiz. **54**, 197 (1991) [JETP Lett. **54**, 193 (1991)].
[16] N. N. Achasov and A. A. Kozhevnikov, Phys. Rev. D **49**, 275 (1994).
[17] N. N. Achasov and A. A. Kozhevnikov, Yad. Fiz. **69**, 1017 (2006) [Phys. At. Nucl. **69**, 988 (2006)].
[18] V. A. Khoze and M. A. Shifman, Usp. Fiz. Nauk **140**, 3 (1983) [Sov. Phys. Usp. **26**, 387 (1983)].
[19] R. A. Briere *et al.*, Phys. Rev. D **74**, 031106(R) (2006).
[20] T. K. Pedlar *et al.*, Phys. Rev. D **79**, 111101 (2009).
[21] N. E. Adam *et al.*, Phys. Rev. Lett. **96**, 082004 (2006).
[22] G. S. Adams *et al.*, Phys. Rev. D **73**, 012002 (2006).
[23] X. L. Wang *et al.*, arXiv:1210.7550.
[24] M. Ablikim *et al.*, Phys. Rev. Lett. **97**, 262001 (2006).
[25] M. Ablikim *et al.*, Phys. Lett. B **652**, 238 (2007).
[26] D. Besson *et al.*, Phys. Rev. Lett. **104**, 159901(E) (2010).
[27] B. Aubert *et al.*, Phys. Rev. D **76**, 111105(R) (2007); Report No. SLAC-PUB-12818, 2007.
[28] B. Aubert *et al.*, Phys. Rev. D **79**, 092001 (2009).
[29] G. Pakhlova *et al.*, Phys. Rev. D **77**, 011103 (2008).